Analysis of backwash settings to maximize net water production in an engineering-scale ultrafiltration system for water reuse

Mohammed A. Alhussaini[a,b], Zachary Binger[a,b], Bianca M. Souza-Chaves[a,b], Oluwamayowa Amusat[c], Jangho Park[c], Timothy V. Bartholomew[d], Daniel Gunter[c], Andrea Achilli[a,b*]

[a]Department of Chemical and Environmental Engineering, University of Arizona, Tucson, AZ, 85721, United States
[b]Water and Energy Sustainable Technology (WEST) Center, University of Arizona, Tucson, AZ 85745, United States
[c]Lawrence Berkeley National Laboratory, Berkeley, CA 94720, United States
[d]National Energy Technology Laboratory, Pittsburgh, PA 15236, United States

[*]Corresponding author:
Andrea Achilli: achilli@arizona.edu

Prepared for submission to *Journal of Water Process Engineering*

Abstract

Ultrafiltration (UF) has been widely utilized as water pretreatment for different applications especially in water reuse. The UF system operation is characterized by a filtration phase, where particles accumulate on the membrane surface resulting in an increase in the transmembrane pressure (TMP) and a cleaning phase, where foulants are removed through cleaning cycles including physical backwash and chemical enhanced backwash (CEB). In this study, data from an engineering-scale UF system treating reclaimed wastewater were used to assess the impact of backwashing on the filtration process. TMP backwash trigger, backwash duration, and CEB frequency were purposely varied for a cycle-by-cycle investigation on the net water production, water recovery, initial operating TMP, and filtration cycle duration. As the TMP backwash trigger was varied between 62 and 145 kPa, the maximum net water production (63 m^3/d) was achieved at 103 kPa and water recovery remained relatively constant at approximately 92%. Backwash durations of 45, 65, and 85 seconds were performed where both net water production and water recovery yielded similar results (~63 m^3/d and ~91%) compared with 103 kPa TMP backwash trigger. The CEB frequency was also lowered from one every three backwashes (1/3) to 1/6 and 1/12 and resulted in decreased net water production and water recovery while the initial TMP increased. Interestingly, the total number of CEBs remained approximately constant regardless of their frequency. Results suggest that CEB is an important fouling control process to maximize water production.

Keywords: ultrafiltration; water reuse; membrane fouling; backwash; data mining.

1. Introduction

Membrane-based processes are currently the leading technologies for sustainable water production for a wide variety of applications, including water reuse. Membrane processes including ultrafiltration (UF) [1, 2], nanofiltration (NF) [3-5], reverse osmosis (RO) [6-8], forward osmosis (FO) [9-11], and membrane distillation (MD) [12-14] are well-researched technologies at different stage of development that are present in the water treatment and reuse research field for both potable and non-potable applications. Water reuse is one of the unconventional water resources that has been expanding rapidly to overcome the increased demand for clean water [15, 16]. In the last few decades, advanced treatment and membrane systems have been adopted when physical space is limited, and water reuse is being considered [17, 18]. Full advanced treatment (FAT) is an effective barrier against salinity, organic pollutants, and pathogens and has emerged as a state-of-the-art technology for water reuse applications. FAT is a multi-barrier treatment system that includes MF/UF, RO, and advanced oxidation processes (AOP) [19]. The FAT system produces high-quality water, removing pathogens as well as physical and chemical constituents to meet water quality limits. UF is an essential part of FAT systems and has been increasingly implemented as pre-treatment for wastewater treatment and recycling, including water reuse applications [15]. UF membranes are versatile and have been extensively applied in combination with different processes such as membrane bioreactors [20], reverse osmosis membrane pre-treatment [21, 22], and before/after biological aerated filters [23]. UF membranes provide an effective barrier to the removal of particles, suspended/colloidal compounds, and micro-organisms, delivering high-quality effluent compared to conventional pre-treatment methods [24].

Although UF has become a major component in most water reuse treatment schemes, the operation, monitoring, and cleaning pose unique challenges to the process, mainly from membrane fouling [2, 25]. Even though precipitation and deposition of particulates on the membrane pores/surface could be alleviated by physical and chemical cleaning, membrane fouling is still a complex phenomenon governed mainly by operating conditions, membrane characteristics, and feed water quality [26, 27]. Fouling buildup on the membrane surface increases membrane resistance, restricts water productivity, and challenges sustainable operations. In addition, besides limiting water production, fouling also increases the cleaning frequency, energy consumption, and consequently, operating costs [28, 29]. In water reuse applications, UF fouling is caused by major potential foulants such as microbes, natural organic matter, inorganic, and colloidal content [29-

31]. In addition, during fouling progression, there are several types of fouling mechanisms typically observed. The main mechanisms can be described as: (i) complete blocking, when molecules are larger than the membrane pores and block the fluid passage, (ii) standard blocking, when molecules are smaller than the membrane pore size and accumulate on the pore walls (pore constriction), (iii) intermediate blocking, similar but less restrictive than the complete blocking mechanism, when some molecules block the membrane pores, while others deposit on molecules already accumulated on the membrane surface, and (iv) cake filtration, when molecules are deposited on the membrane surface in a permeable cake layer of crescent thickness [32, 33]. Hlavacek and Bouchet developed a blocking law equation that describes fouling mechanism type at constant-flux dead-end filtration [34]. These fouling mechanisms can occur individually or simultaneously during the UF filtration. Each mechanism has a signature impact on the loss of process performance (e.g., water production) [35]. Nevertheless, in the UF process, especially dead-end mode, complete pore blocking and cake filtration are the dominant fouling mechanisms [30, 32, 36].

The operation of a UF system is commonly characterized by a series of cycles, where each cycle has two operating phases: a filtration phase, where foulants accumulate on the membrane surface, increasing the transmembrane pressure (TMP) in a dead-end and constant-flux operation mode; and a cleaning phase, where the foulants are removed through backwash cleaning methods including physical backwash, chemical-enhanced backwash (CEB), and chemical clean-in-place (CIP). Filtration and backwash cycles alternate to produce the desired filtrate. The physical backwash cycle is an intermittent routine process that takes place after each filtration cycle and is triggered by a set filtration duration or by a set TMP value (i.e., the maximum filtration pressure that when is reached triggers the start of the backwash cycle). The physical backwash includes air scouring and a subsequent reversed filtration flux to unblock the fiber's pores and clean the membrane and thus remove reversible fouling. However, due to the gradual accumulation of irreversible fouling over several filtration cycles, a CEB cycle is used to achieve deeper membrane cleaning and minimize irreversible fouling [37]. Usually, a CEB cycle is operated on a periodic automatic sequence initiated after a predefined number of physical backwash cycles where it involves soaking the membrane for several minutes in a low concentration of a chemical solution (e.g., sodium hypochlorite, sodium hydroxide, or hydrochloric acid). The physical and/or chemical reaction between chemical agents and foulants helps remove fouling and avoid microorganisms'

growth on the membrane surface and inside the pores [38, 39]. Furthermore, the progressive buildup of irreversible fouling not removed by physical backwash or CEB leads to water production decline over time because of long-term increase in operating TMP that maintains the desired constant flux requiring CIP. In the CIP process, the membrane has a longer contact time with chemical solutions, typically several hours, to reduce long-term irreversible fouling and restore initial operating TMP and water productivity. Both physical backwash, CEB, and CIP methods utilize a portion of stored UF-filtrate for cleaning. Therefore, excessive cleaning can largely reduce water recovery, increase energy consumption, and increase cost, which pose challenges to sustainable UF water production. However, less frequent backwashing can lead to a higher fouling buildup rate that reduces the UF filtration cycle duration and therefore decreases net water production. In addition, it is important to note that the membrane structure could be damaged as a result of more frequent CEBs, altering the permeability and selectivity of the membrane [40, 41].

UF fouling has been a major interest area in the last few years. Numerous studies have focused exclusively on UF membrane fouling on lab-scale [42-46] and only a few on pilot and engineering-scale systems [46-50]. As membrane fouling is primarily affected by backwash conditions (e.g., flow rate, pressure, frequency, and chemical dosing); studying the influence of these parameters provides a better assessment of UF operation, primarily net water productivity. Accordingly, various efforts have been made to enhance the UF filtration process by investigating the backwash methods including backwash water composition [25, 51-54], additional air sparging steps [55-58],use of different chemical cleaning agents [38, 39, 59, 60], and in-line pre coagulation [61-65]. Most previous works, however, have focused on short-term single or multiple experiments using synthetic water. A knowledge gap exists in assessing the long-term impact of filtration and backwash, and the need for cycle-by-cycle and data mining analysis for a continuous engineering-scale system treating reclaimed wastewater. Cycle-by-cycle analysis is a method of monitoring the parameters of the UF system by mining the whole raw data generated and analyzing the UF process on a cycle-by-cycle basis (filtration, backwash, and CEB). In addition, unlike pilot-scale, an engineering-scale system is a system representative of full-scale, which is fully automated, monitored, and operated continuously. Although the availability and complexity of water system datasets can be challenging, cycle tracking and data-driven analysis of raw operational data can help spot and identify any faults or irregularities [66-68]. The data management analysis helps

organize and examine the overall state of operating conditions with the goal of optimizing the UF parameters, while long-term cycle-by-cycle monitoring can provide a detailed assessment of the UF system operation behavior.

In this study, an engineering-scale UF system treating reclaimed wastewater was used to determine how TMP backwash trigger, physical backwash duration, CEB frequency, and chemical dosage variations influence the net water production, operating TMP, and energy consumption of the UF system. This study takes advantage of operational data generated by the engineering-scale UF system. Week-long experiments were conducted to isolate the effect of operating parameters in a cycle-by-cycle analysis allowing a detailed investigation of the net water production, water recovery, initial operating TMP, and filtration cycle duration, as well as to identify the mechanisms and rate of fouling were also assessed during the filtration process. This study presents a first step to develop a data management procedure for monitoring cycle-by-cycle behavior, in which net water filtrate, filtration cycle duration, and initial TMP serve as UF operation metrics and fouling indicators.

2. Materials and Methods

2.1. Engineering-scale ultrafiltration system

The engineering-scale UF system (Figure 1) is part of a UF-RO water reuse train (Applied Membranes, Inc., Vista, CA, USA) that can treat up to 75 cubic meters per day of reclaimed wastewater. The UF engineering-scale system has been operating continuously for more than three years at the Water & Energy Sustainable Technology (WEST) Center at the University of Arizona in Tucson, Arizona (USA). It is composed of one DOW IntegraFlux module UXA-2680XP hollow fiber polyvinylidene fluoride (PVDF) UF membrane (55 m^2 active area, nominal 0.03 μm pore diameter) operated in a dead-end outside-in filtration mode with a constant instantaneous flow of 53 liters per minute (57.8 L/m^2 h water flux). Reclaimed wastewater is pretreated with 90 and 140-mesh (162 and 104 μm) screen filters in series before entering the UF feed tank and two 100-mesh (152 μm) screen filters in parallel prior to the UF module. UF filtrate is used for backwash. For CEBs, two chemical dosing pumps utilizing sodium hypochlorite and sodium hydroxide are used. The UF system is fully automated and constantly monitored. Both UF feed and filtrate samples are collected periodically for water quality analysis.

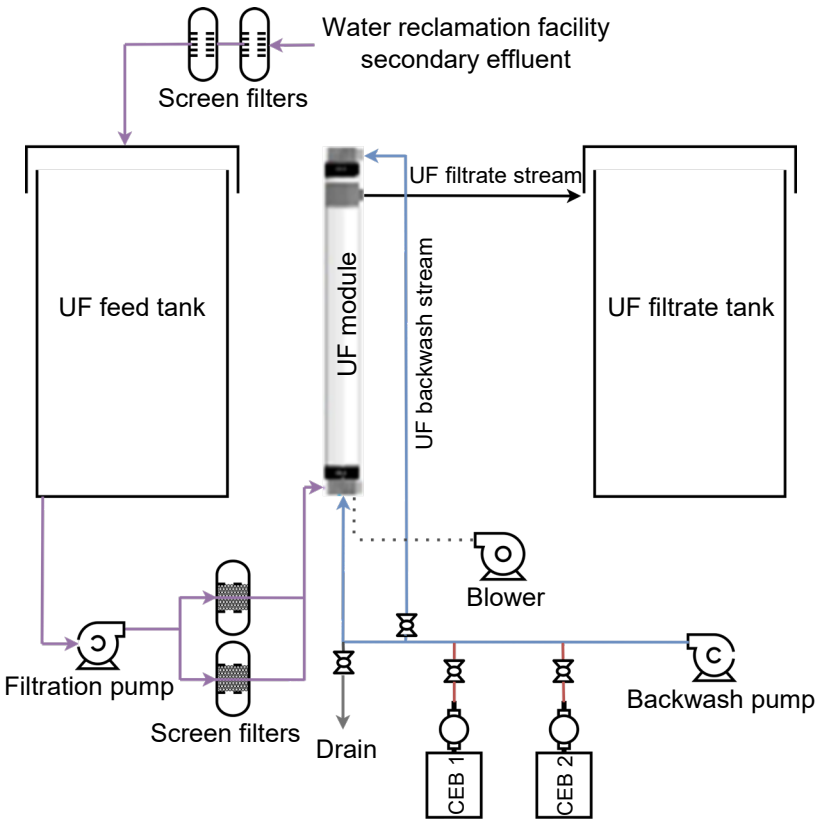

Figure 1. Schematic of the ultrafiltration engineering-scale system

2.2. Reclaimed wastewater

Treated wastewater effluent from Pima County's Agua Nueva Water Reclamation Facility (five-stage Bardenpho wastewater treatment system bioreactors and clarifiers, disk filters, and chlorination) was passed through two screen filters before being pumped directly to the UF system. The average intake reclaimed wastewater quality is shown in Table 1.

Table 1. UF feed and filtrate water quality

Water quality parameter	**UF feed**	**UF filtrate**
Turbidity (NTU)	0.7 - 1.0	0.1 - 0.2
pH	7.0 - 7.3	7.0 - 7.3
TDS (mg/L)	650 - 700	650 - 700
TSS (mg/L)	1.0-1.1	0.1 - 0.15
Total fluorescence (10^9 R.U. nm^2)	10 - 30	1 - 2
TOC (mg/L)	8-11	5-7

2.3. Physical backwash and chemical-enhanced backwash (CEB)

The physical backwash cycle occurs when the filtration operating TMP exceeds a predetermined TMP set-point. For CEBs, two chemicals were used, sodium hypochlorite (6% v/v, NaClO, Kroger, Cincinnati, OH) for CEB-1 and sodium hydroxide (50% w/v NaOH; >99% purity, Duda Energy LLC, Decatur, AL) for CEB-2. CEB-1 cycle is initiated after three physical backwashes, and CEB-2 is triggered after two CEB-1 cycles. Both physical backwash and CEB cycles automatic sequences are shown in Table 2. UF-filtrate stored in the filtrate tank was used for both physical backwash and CEB cycles.

Table 2. UF initialization control strategy sequence

START UF
UF 1: Forward Flush
UF 2: Reaching Target Flow
UF 3: ONLINE
Physical Backwash
BW 1: Air scouring
BW 2: Drain
BW 3: Top backwash
BW 4: Bottom backwash preparation
BW 5: Bottom backwash
BW 6: Backwash decompression
Proceed to START UF, STOP UF or CEB
Chemical-enhanced backwash
CEB 1: Top flushing with chemicals
CEB 2: CEBn flushing the top
CEB 3: Soaking
CEB 4: Top chemical rinsing
CEB 5: Bottom chemical rinsing
CEB 6: Preparation for cycle end
Proceed to UF START or STOP UF

2.4. Data mining

A supervisory control and data acquisition (SCADA) and programmable logic controller (PLC) systems of the engineering-scale UF system were used to control and monitor the operating conditions with data recorded every five seconds and then saved to the terminal computer. Table 2 describes the UF PLC control strategy with a predefined time. Preparing raw data for analysis involves data pre-processing, which includes extracting, aggregating, and cleaning the data. A large amount of raw data is recorded for each experiment. Once the data is extracted, it is then pre-processed and analyzed with a Python script developed for the UF system. This pre-processing script breaks down the operational data of the UF process events into three phases: filtration, backwash, and CEB, based on the UF initialization control strategy sequence allowing to determine the operational outputs (total water production, net water production, duration, etc.). In addition, pre-processing checks for general data quality, flags errors and inconsistencies in the experimental data (if any) and converts the data into a more human-interpretable form for further analysis. Data pre-processing is used to ensure that outliers' readings of sensors not involved with the proper state of operation are ignored. For example, noise in the sensors measuring the flow rates may result in a small reading even during times of non-operation. Typically, these sorts of readings can be ignored; however, due to the timescale of this analysis, these errors can accumulate into a measurable magnitude which can cause incorrect reporting of system performance. Furthermore, any gaps in data greater than 10 seconds due to logging errors in the system, were backfilled using the average value of each parameter.

2.4.1 Splitting data into cycles and identification of operating regimes

The UF system reports instantaneous data; however, data were grouped and utilized in multiple timescales including instantaneous/raw, single filtration cycle (time between physical backwashes), and daily intervals. The length of the cycles was determined by tracking the changes in the value of the UF start-up variable. Once the cycles have been identified, each measurement within the cycle was annotated with information about the current state of the system. The four potential operating stages were identified (filtration, physical backwash, chemical-enhanced backwash with NaClO or NaOH, and system off). The operating flow chart of UF processes is shown in Figure 2. Information about the total time spent in each state within the cycle is also documented, allowing us to compute the cycle-by-cycle and operational duration.

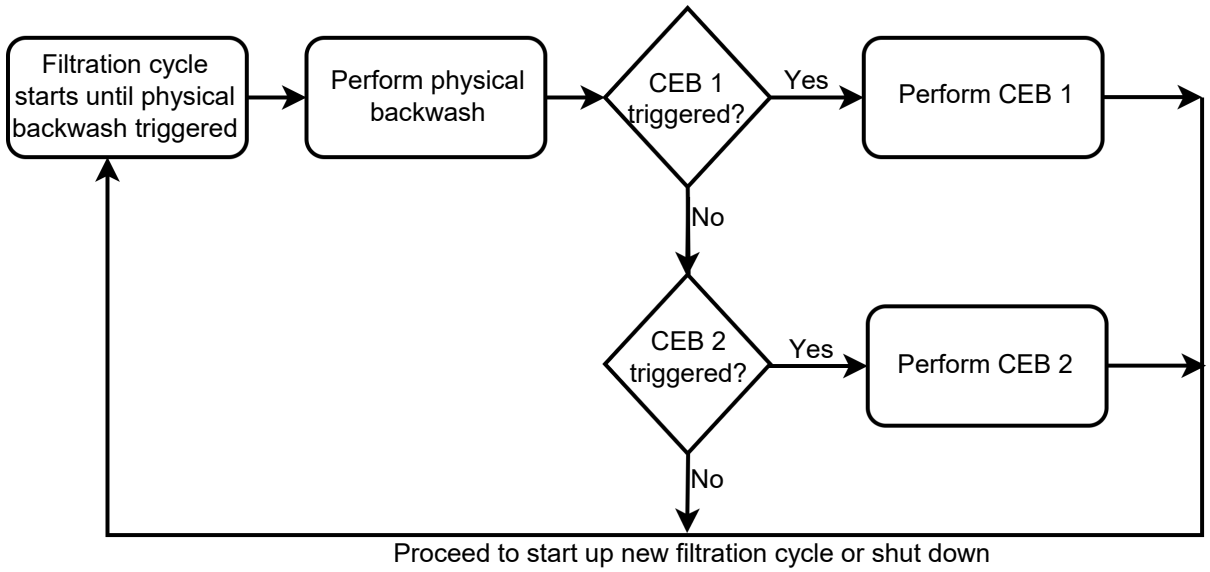

Figure 2. UF process flow diagram

As each UF sequence (filtration, physical backwash and CEB cycles) with different steps is recorded and given unique ID, all raw data were separated and tabulated. Each sequence and step are identified and quantified for cycle-by-cycle analysis of total and net water production, water recovery, cycle duration, and initial operating TMP. The net water production is calculated as:

$$Net\ water\ production = V_f - V_{BW} - V_{CEB} \quad (1)$$

where V_f is the total filtrate volume, V_{BW} is the filtrate volume used during physical backwash, and V_{CEB} is the filtrate volume used during chemical-enhanced backwash. The water recovery is calculated as the ratio between net water production and total water production. The initial operating TMP value was selected at the start of the filtration cycle. For each set of experiments, net water production, water recovery, initial operating TMP, and cycle duration were calculated for each cycle through the period of the experiment then a daily average was calculated.

2.4.2 Backwash trigger identification

The backwash cycle is triggered when the UF TMP exceeds the set-point. However, initial analysis of the recorded data revealed that the backwash was triggered below the set-point of the TMP on several occasions during the UF cycle. Further analysis of those specific cases revealed that the physical backwash was initiated because the water storage tank was full. Identifying the trigger for the backwash is important since it directly impacts the duration and productivity of the filtration cycle. When the physical backwash is triggered because of the tank level, the filtration

cycle is terminated mid-operation before the TMP set point is reached, leading to reduced water production. To keep track of this, each filtration cycle within the dataset was annotated as either "TMP-triggered" or "tank-level triggered" based on the TMP value at the end of the filtration cycle. The total, net, and daily averaged water production, water recovery, and filtration cycle duration were computed.

2.5. UF fouling mechanisms

The fouling mechanism of constant flow rate dead-end UF was analyzed using the blocking laws [34, 69]:

$$\frac{d^2P}{dV^2} = k\left(\frac{dP}{dV}\right)^n \quad (2)$$

where P is the transmembrane pressure, V is the cumulative filtrate volume, k is the fouling coefficient, and n is the fouling index. The fouling index describes the type of fouling mechanism, with n = 2 for complete blocking, n = 1.5 for standard blocking, n = 1.0 for intermediate blocking and n = 0 for cake layer [33]. The fouling index can be obtained from the slope of the logarithmical plot of d^2P/dV^2 as function of dP/dV. The first and second derivatives were calculated based on numerical differentiation of experimental data. Furthermore, as the first derivative indicates the TMP variation, a rapid change in the second derivative suggests a potential fouling mechanism shift during filtration.

2.6. Experimental protocols

The engineering-scale UF system was used to conduct a week-long experiment for each of the different TMP backwash trigger, physical backwash duration, CEB frequency, and chemical dosage conditions. First, five TMP backwash trigger conditions of 62, 82, 103, 124, and 145 kPa (9, 12, 15, 18, and 21 psi) were tested with a fixed physical backwash duration of 65 seconds. From these experiments, the TMP trigger condition that resulted in the highest net water production was selected for the next set experiments. Using the TMP trigger condition of the highest net water production from the first set of experiments, a second set of experiments was conducted where the duration of the physical backwash duration was varied between 45 seconds and 85 seconds. Lastly, a third set of experiments was conducted where the CEB frequency was varied by lowering its frequency from one every three physical backwashes (1/3) to 1/6 and 1/12. Furthermore, the effect of the chemical dosing was tested by running experiments with frequency of (1/6) with no chemicals used in the CEBs. Throughout all the experiments, the filtrate flow rate

and physical backwash flow rate was constant at 53 and 114 L/min (14 and 30 gallon/min) respectively.

2.7.Specific energy consumption

The engineering-scale UF system electricity usage (kWh) was obtained from data recorded daily by a power meter. The volume of UF feed water was recorded by a water flow meter (Carlon Meter, Grand Haven, MI). The actual specific energy consumption (SEC_a) of the UF system was calculated in kWh/m^3 as:

$$SEC_a = \frac{Energy\ used}{Q_f} \tag{3}$$

where Q_f is the UF feed water flow rate. In addition, the theoretical specific energy consumption (SEC_{th}) of the filtration process was calculated as:

$$SEC_{th} = \frac{\sum(Q_f * TMP)}{\sum(Q_{fil})} \tag{4}$$

where Q_{fil} is the UF filtrate flow rate.

3. Results and Discussion

3.1. Filtration cycle length and transmembrane pressure trigger

As the TMP backwash trigger was varied between 62 and 145 kPa (9 and 21 psi) – hypothesizing that higher pressure would allow for longer filtration time – the filtration time increased as the TMP backwash trigger increased only up to 103 kPa (15 psi) and decreased afterward (Figure 3a). Also, it was observed that as the TMP backwash trigger increases, the resulting initial TMP also increases, suggesting a fixed TMP recovery amount, which is likely because the backwashing has a fixed level of impact irrespective of the operating TMP. Because the longest filtration time was reached at 103 kPa (15 psi) (45±3 min filtration cycle duration), this TMP value resulted in the condition having the highest net water production (63 m^3/d) and water recovery (Figure 3b). It is worth noting that, while net water production is statistically different for all the TMP backwash trigger conditions, the water recovery remained high and around 90%, which indicates that the system should not only be evaluated based on the water recovery parameter.

(a) (b)

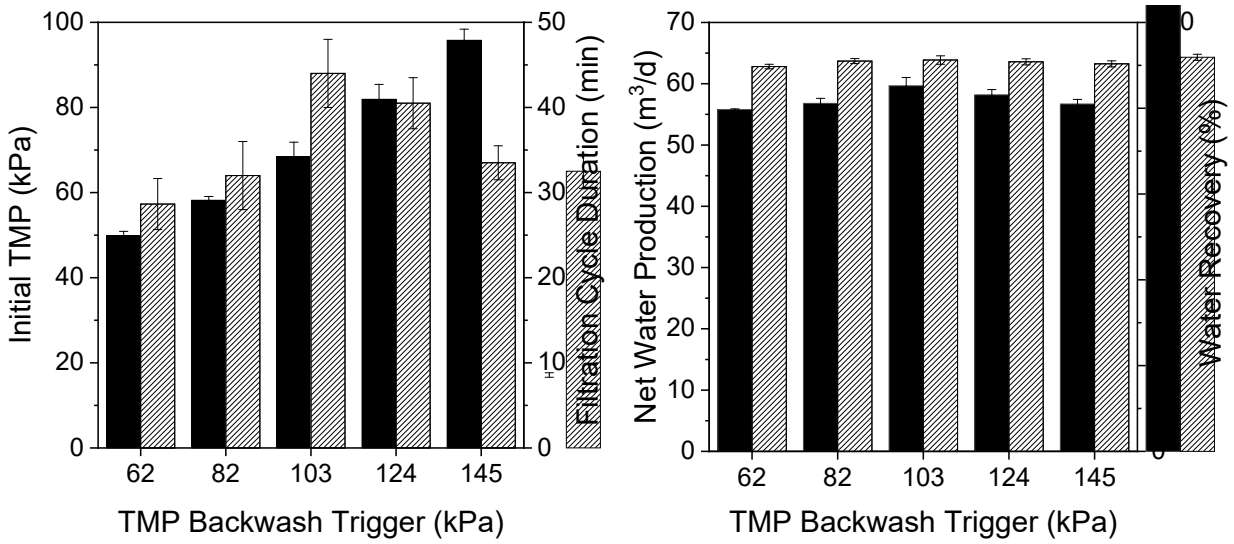

Figure 3. a) Initial operating TMP (■) and filtration cycle duration (▨), and b) net water production (■) and water recovery (▨) correspondent to each TMP backwash trigger conditions tested (62, 82, 103, 124, and 145 kPa). Bars illustrate the calculated daily average values.

The TMP difference between the start and end of filtration cycles can be visualized in Figure 4a. For 62 and 82 kPa (9 and 12 psi) backwash trigger conditions, the TMP difference between the start and end of filtration is relatively constant along the one-week testing period. This suggests that the backwashing setting may have been over-conservative, as the initial TMP after backwashing was constant and similar (approximately 48-55 kPa, 7-8 psi) for both settings. A decrease in the TMP difference was observed over time for physical backwash trigger pressures from 103 to 145 kPa (15 to 21 psi), although these pressures yielded longer filtration duration and higher net water production. This behavior suggests that for the higher TMP backwash trigger conditions, there is a higher fouling accumulation which isn't fully removed by physical backwash. When increasing the TMP backwash trigger, other backwashing parameters (e.g., physical backwash duration or flow rate) should be also altered to completely remove the fouling layer. Moreover, interestingly, when the rate of increase of TMP over time is plotted as function of time (Figure 4b), it can be observed that the foulants accumulation rate is slower during the night than the day. This fluctuation is likely due to variations in reclaimed wastewater composition, which produces a less concentrated effluent (low fouling) during the night.

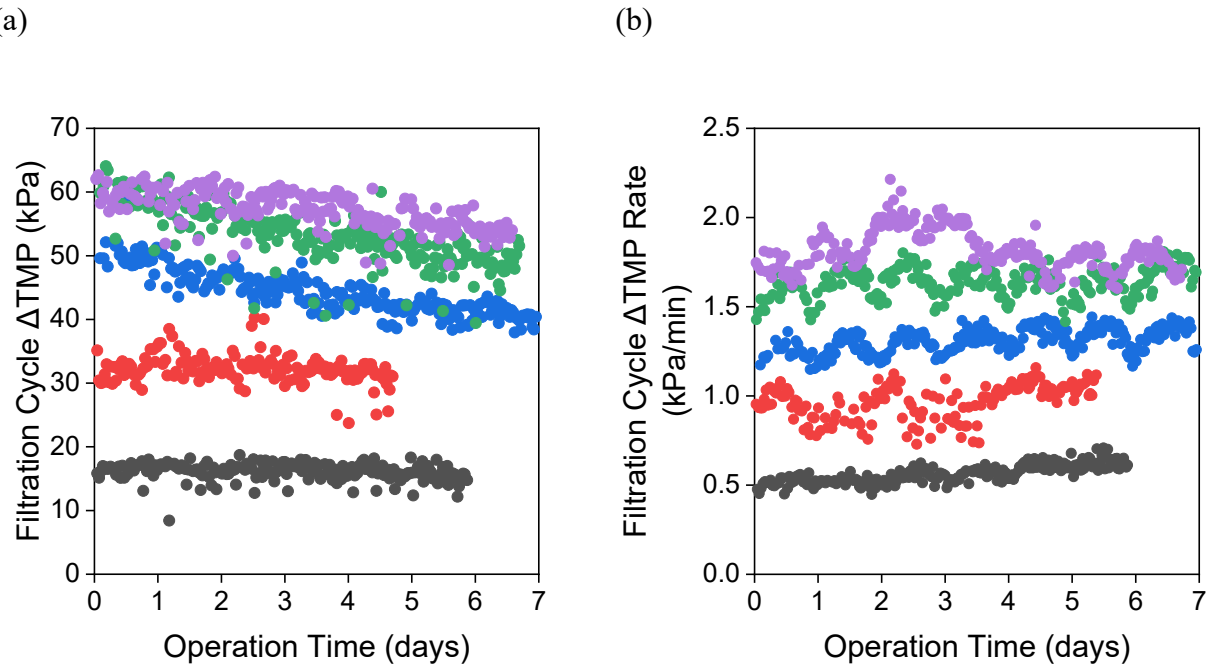

Figure 4. a) TMP difference between the start and end of different cycles, and b) TMP difference rate duration cycle during one week of operation for each backwash trigger conditions. (●) 62 kPa; (●) 82 kPa; (●) 103 kPa; (●) 124 kPa; (●) 145 kPa. Each data point represents one filtration cycle.

3.2. Filtration cycle behavior

The first experiment focused on studying the impact of the TMP backwash trigger condition on UF net filtrate production. UF fouling occurs during filtration and increases the resistance, and fouling is removed to some degree by backwashing. To understand the net water production variation at different TMP backwash trigger conditions, the TMP behavior was analyzed as a function of time for all filtration cycles (Figure 5). Despite having different TMP backwash trigger conditions 62, 82, 103, 124, and 145 kPa (9, 12, 15, 18, and 21 psi), the TMP evolution as a function of time of the different filtration cycles was similar. The minimum pressure was achieved at a TMP backwash trigger of 62 kPa (9 psi), with all the cycles starting at 41 kPa (6 psi). At this point, all the reversible fouling is recovered, and the membrane is considered in a clean state. Increasing the TMP backwash trigger led to an increase in the initial operating TMP of the different TMP trigger experiments for each filtration cycle. In addition, the progressive fouling increases the initial operating TMP even more with time for each experiment. For all tested physical backwash trigger pressures, the membrane could not be restored to its original state, likely due to

irreversible fouling resulting in the reduction in UF backwash effectiveness with time. A portion of the foulants that are not removed by physical backwash would be poorly removed or remain irreversible in the subsequent backwash cycles, in which the accumulation on the membrane surface reduces net water production. This can also be explained as the system backwashing has fixed TMP recovery, which remains constant regardless of the set point increases. From Figure 5, for each TMP trigger conditions (62, 82, 103, 124, and 145 kPa), the average pressure increase between the start and end of a filtration cycle remained approximately constant (21, 28, 41, 48, and 55 kPa) through the duration of the experiment. This behavior is also observed when all cycles are plotted as a function of the filtrate volume (Figure 6). To better illustrate the consistency of the general shape seen for the TMP profiles in Figure 5, the TMP profile for each TMP range is combined into one uninterrupted profile. Each of the resulting uninterrupted cycles is then plotted as a function of filtrate volume to show the consistent overlap and shape of this data. In Figure 6a, the different colors represent each uninterrupted filtration cycle, and it is noted that for all tested TMP set-points the TMP slightly increases at the beginning of the UF operation, likely due to initial membrane stabilization. A rapid increase in TMP is observed as more volume is filtered until it reaches the TMP trigger value. This sharp increase in pressure is likely associated with the particles' deposition on the membrane surface, which consequently increases the membrane resistance. It can also be observed that this behavior is persistent and independent of the TMP trigger condition. All the TMP profiles in Figure 6a were then averaged and curve-fitted to create a TMP profile that represents the average behavior of all filtration cycles throughout the entire TMP range (Figure 6b). All cycles of all different TMP backwash trigger conditions tend to have uninterrupted TMP profiles, which generates one overall cycle. The effect of the different TMP backwash trigger conditions, different CEB frequencies, and dosing can be seen from the upper and lower bound as cycles start at different TMP.

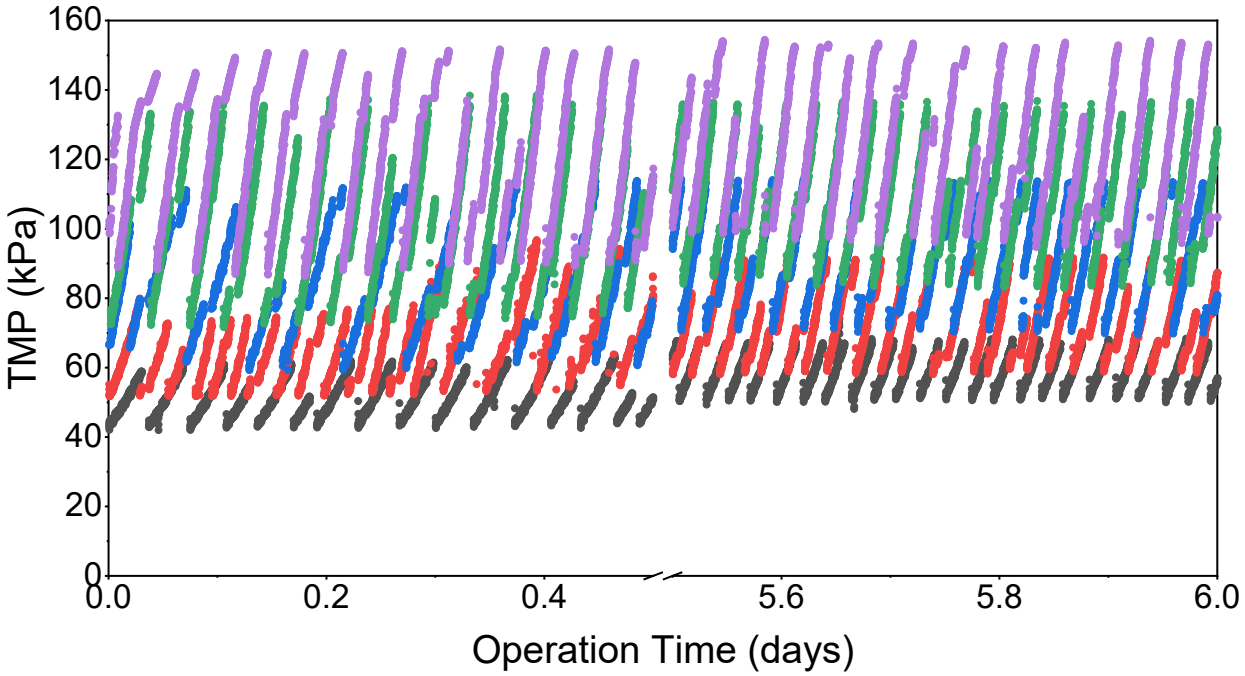

Figure 5. Illustration of UF operation displaying instantaneous TMP profiles during filtration cycle for each TMP backwash trigger conditions as a function of operation time (●) 62 kPa; (●) 82 kPa; (●) 103 kPa; (●) 124 kPa; (●) 145 kPa.

(a) (b)

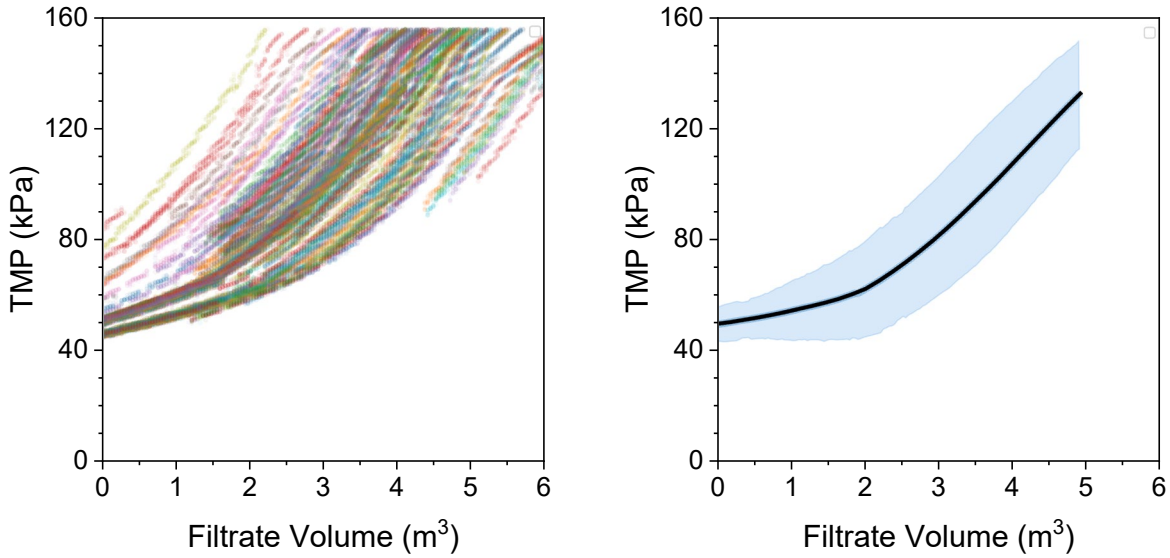

Figure 6. a) TMP profile for all filtration cycles and b) unified filtration cycle TMP profile with error bands (showing one standard deviation from the mean) as a function of filtrate volume.

3.3. UF fouling mechanisms

To analyze the fouling mechanisms, data from Figure 6b was plotted as first and second pressure derivative with respect to filtrate volume (Figure 7). As shown in Figure 6b, an initial slow gradual increase in TMP was observed for filtrate volume up to 2 m^3, but then the rate increased rapidly (to 4.5 m^3). Similarly, in Figure 7a, it is observed that *dP/dV* gradually increases at short filtration volumes (up to 2 m^3), and then increased exponentially at long filtration times until it reaches a maximum value at filtration volume of 4.5 m^3, after which the TMP variation rate starts decreasing. This negative slope can represent a direct transition from pore blockage to cake-layer filtration in UF membranes [70]. Also, it is reported that organic fouling usually occurs in three stages: pore blocking, cake filtration without compression, and cake filtration with compression [71]. Therefore, the observed occurrence suggests that the increase in resistance at the initial stage of filtration sharpens the slope mainly due to pore blocking increase, and the change from positive to negative slope in the final period is likely related to the cake filtration mechanism formation [72, 73]. Illustrated in Figure 7b, the second derivative resulted in a complex behavior which cannot be explained by the classical blocking filtration law represented by Eq. (2). This fluctuating behavior complements the hypothesis that combined effects of different individual fouling mechanisms may be occurring. The rapid change in the second derivative suggests a dominant fouling mechanism and a shift from one mechanism to another can be noted when the d^2P/dV^2 changes from positive to negative values.

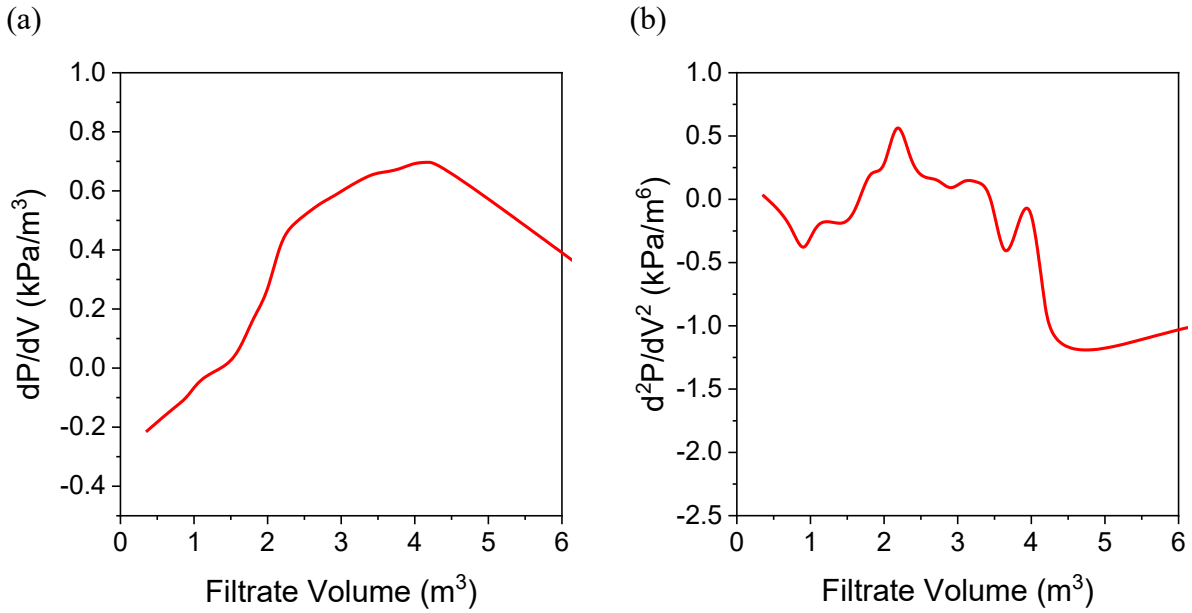

Figure 7. Rate progression of TMP a) TMP first derivative and b) TMP second derivative as a function of filtrate volume. The red line represents the derivative rate change over volume produced.

To further identify the dominant fouling mechanism and/or if a fouling mechanism transitioned from one to another in each experimental period, the logarithmic values of the second derivative were plotted as a function of the first derivative (Figure 8) and the blocking laws were used to fit the results. Therefore, the characteristic slope (fouling index) of filtration data was analyzed based on the classical blocking laws. The slope value (n) is close to two at the early filtration stage, indicating that a complete pore blocking mechanism is taking place. As the filtration proceeds, the fouling index becomes equal to zero, indicating a transition from complete pore blocking to cake layer. Since the engineering-scale system has been operating for three years prior to these experiments, the membrane pore area availability was likely reduced over time due to irreversible fouling. Considering that the complete pore blocking mechanism is associated with molecules larger than the membrane pore size, the reduction in UF effectiveness during the cycles is probably related to the deposition of particles larger than 0.03 µm on the membrane surface, therefore the fouling mechanism is not initiated by internal pore fouling, but surface fouling (pore blocking) that later is transitioned to cake layer.

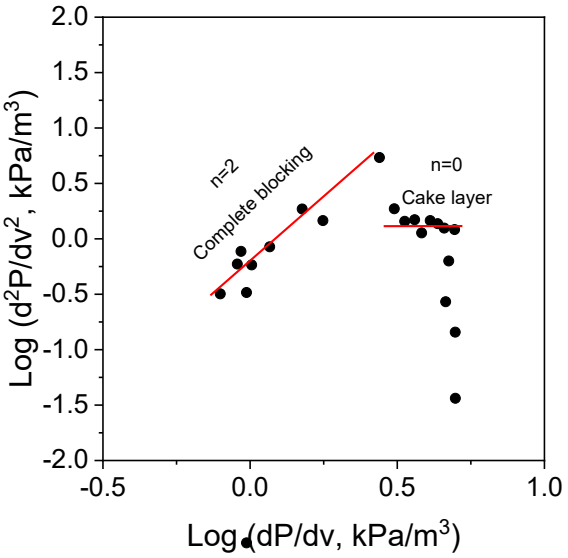

Figure 8. Constant flux blocking law analysis of the unified cycle data points. Red lines represent average slope value of derivative points indicating fouling mechanism initiated as complete blocking (slope of 2) then transitioned to cake layer (slope of 0).

3.4. Backwash duration

Considering that the highest net water production and longest filtration cycle duration were achieved at 103 kPa (15 psi) with a backwash duration of 65 seconds, this TMP setting was selected for additional experiments. The tests were performed with a shorter (45 seconds) and a longer (85 seconds) backwash duration and compared with the original backwash duration (65 seconds) (Figure 9). Increasing the backwash duration had relatively small increase on both initial TMP and filtration cycle duration (Figure 9a). Approximately the same net water volume (4.5 m^3/d) was produced at different backwash duration, and with similar water recovery rates (~91%), suggesting that 45 seconds backwash period is adequate (Figure 9b). Overall, unnecessary backwashing cycles wastes both filtration volume and operation time and increases the overall energy consumption.

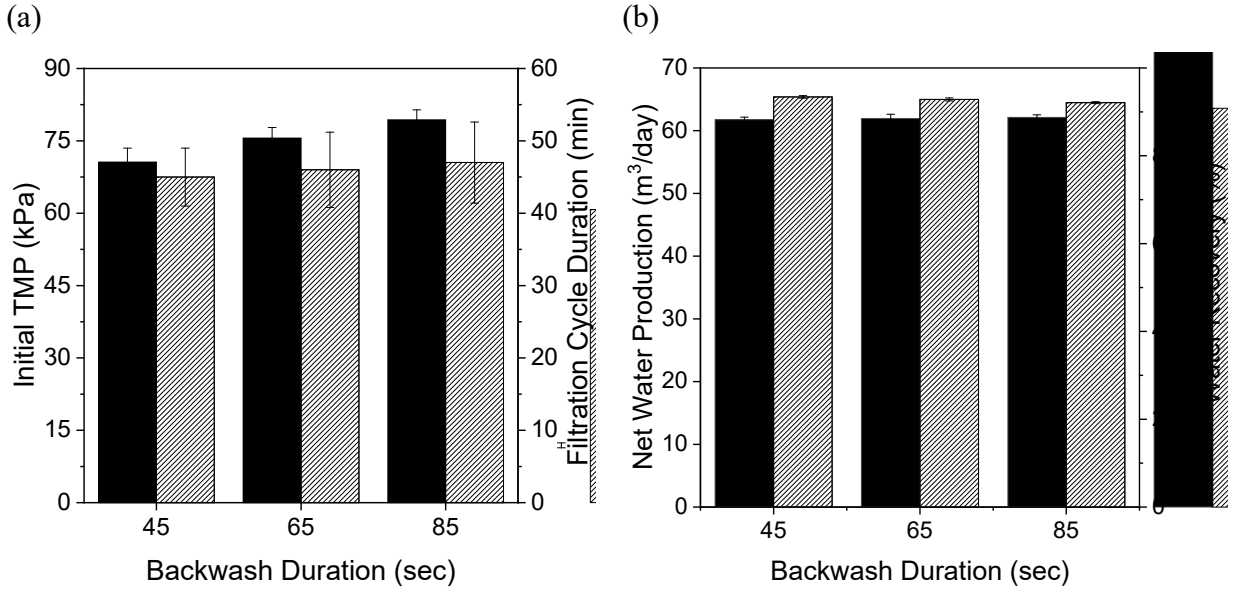

Figure 9. Impact of different backwash duration tested (45, 65 and 85 seconds) on a) initial operating TMP (■) and filtration cycle duration (▨) as function of backwash duration, and b) net water production (■) and water recovery (▨). Bars represent daily average values

3.5. Chemical-enhanced backwash (CEB) frequency

The CEB frequency was varied by lowering the frequency from one every three physical backwashes (1/3) to 1/6 and 1/12. Also, the absence of the chemical dosing was tested with 1/6 of physical backwashes and results are presented in Figure 10. As illustrated in Figure 10a, reducing the CEB frequency increases the initial operating TMP and decreases filtration cycle duration.

Decreasing the CEB frequency from 1/3 to 1/12 resulted in the cycle duration to decrease from 48 to 22 minutes and the initial TMP to increase from 76 to 90 kPa (11 to 13 psi). As expected, a less frequent CEB allows for longer build-up of biofouling on the membrane surface which is not removed as easily/quickly (hence the higher TMP). Furthermore, both net water production and water recovery decreased with less frequent CEB (Figure 10b). The lowest water production and recovery were obtained when no chemicals were utilized in the CEBs. Interestingly, because of the shorter filtration cycles, the number of CEBs during the testing period were approximately the same regardless of their frequency (Table 3), except for the no chemical dosing (ND) test. This is important evidence that CEB is an essential operating parameter to maximize water production and recovery.

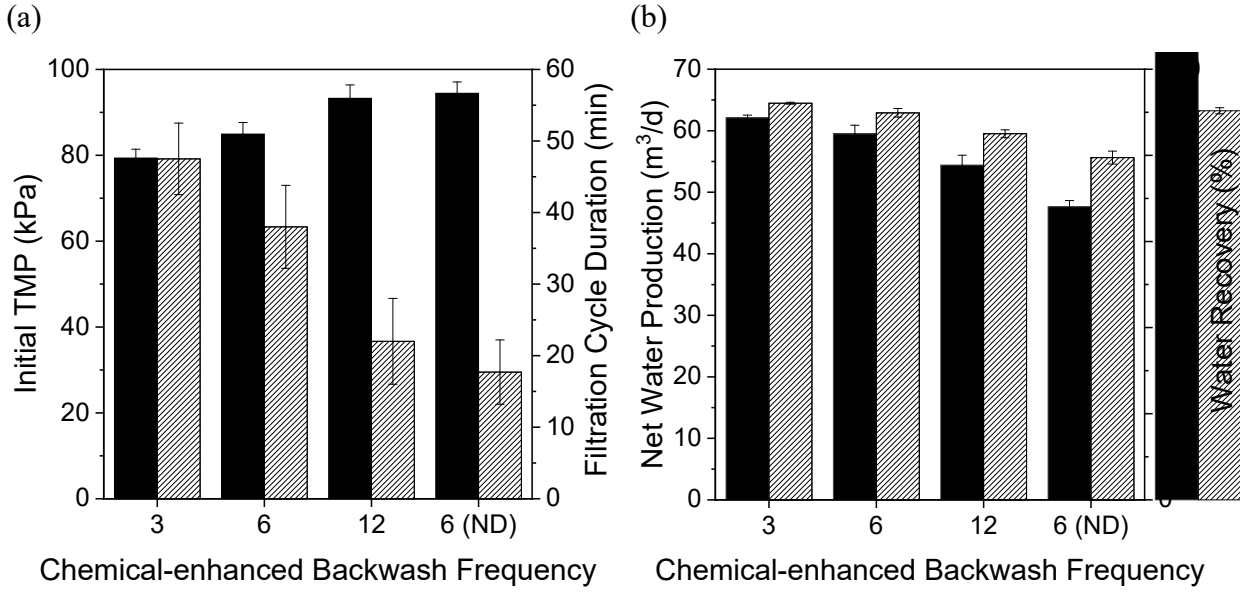

Figure 10. Dependence of a) initial operating TMP (■) and filtration cycle duration (▨), and b) net water production (■) and water recovery (▨) on the different chemical-enhanced backwash (CEB) frequencies tested. Bars illustrate the daily average data.

Table 3. Number of physical and chemical-enhanced backwashes for different frequencies.

Chemical-enhanced backwash frequency	Number of physical backwashes	Number of chemical-enhanced backwashes
3	187	41
6	224	37
12	373	36

6 (No chemical dosing)	415	96

Illustrated in Figure 11 is the impact of the CEB frequency on the filtration cycle durations over time. The filtration cycle duration is inversely proportional to the CEB frequency; higher CEB frequencies restore the operating TMP to lower initial values and thus result in longer filtration cycle durations. However, as the length of time from the last CEB event increases, the filtration cycle duration gets shorter. In addition, in the absence of chemical dosing, there was no difference between the filtration cycles duration since the initial operating TMP after backwashing remained high, causing each subsequent filtration cycle duration to be shorter. Furthermore, the CEB experiments were tested at a fixed duration, and the results suggested that CEB frequency appears to greatly influence the fouling rate. However, CEB duration is another parameter that could be adjusted to improve the effectiveness of the CEB cycle. This finding agrees with previous literature that CEB has a large impact to prevent fouling build up and maintain permeability in UF membranes [41, 74].

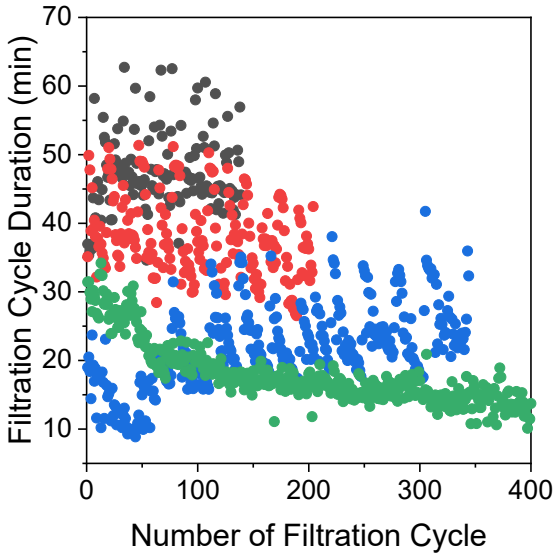

Figure 11. Filtration cycle duration of each cycle for different CEB frequencies. (●) 1/3; (●) 1/6; (●) 1/12; (●) 1/6 No chemical dosing (ND). Data point illustrate the effect of CEB frequencies on the duration filtration cycles.

3.6. Specific energy consumption

In dead-end ultrafiltration, a lot of energy is consumed during both the filtration and backwash processes. The main energy-consuming components in UF systems are the feed pump, backwash

pump, and air blowers, and typical energy consumption values range between 0.1 and 0.4 kWh/m^3 [75]. Illustrated in Figure 12 is the actual and theoretical specific energy consumption for each studied TMP backwash trigger. In general, for all studied conditions, the actual UF SEC ranged from 0.3 to 0.4 kWh/m^3, and 0.34 kWh/m^3 for the longest filtration cycle (103 kPa). As expected, UF energy consumption increases as TMP backwash trigger increases primarily in proportion to the higher operating pressure, and thus more energy is consumed. Moreover, the SEC_{th} ranged from 0.018 to 0.038 kWh/m^3. Although the SEC_{th} results were approximately ten times less than the actual specific energy consumption, they followed the same trend as a function of the TMP backwash trigger. This difference is because rather than considering the whole UF system (air blower, chemical dosing pumps, SCADA system, etc.) the theoretical energy consumption only accounts for the filtration process.

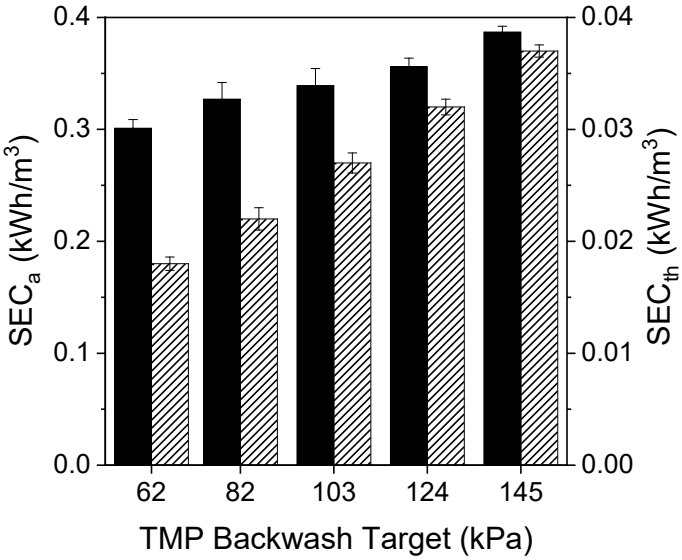

Figure 12. Actual (■) and theoretical (▨) specific energy consumption of the UF as a function of the TMP backwash trigger tested (62, 82, 103, 124, and 145 kPa).

4. Conclusion

UF is increasingly used in various water industries, however membrane fouling challenges its permeability and efficiency. To overcome this challenge, it is important to monitor UF systems' filtration and backwashing cycles. Cycle-by-cycle analysis of UF system data is an essential approach to identify influential parameters that affect the productivity and effectiveness of the UF system and detect any changes over time. This approach allows for real-time adjustments to optimize the system and maintain high production. In this study, a continuous engineering-scale

UF system treating reclaimed wastewater was used to conduct a series of long-term experiments investigating the impact of different operating conditions in cycle-by-cycle analysis to evaluate UF net water production variation and maximize water recovery using different backwash cleaning strategies. Experimental results showed that the 103 kPa (15 psi) TMP backwash trigger yielded the highest net water production (63 m^3/d) with a water recovery of 92%. Moreover, the potential fouling mechanism transitioned from pore blocking to cake filtration. As a result of the gradual accumulation of the suspended particulates on the membrane surface, the fouling mechanism shifts to cake formation faster. Meanwhile changing the backwash duration resulted in only a minimal increase on cycle duration and the net water produced was slightly decreased. In addition, the CEB frequency was a key parameter to maximize water production and recovery and confirmed that chemicals are necessary to maintain robust operation. Moreover, a high dependance of the actual specific energy consumption (0.3 to 0.4 kWh/m^3) was observed as TMP backwash trigger increased (62 to 145 kPa). UF net water production or TMP deviation is a long-term process that should be addressed and studied in an engineering-scale system with real water considering all data generated. This study highlights the importance of cycle-cycle assessment to explore the most influential parameters and enhance UF filtration and backwash to achieve the desired productivity.

5. Declaration of Interests

The authors declare that they have no known competing financial interests or personal relationships that could have appeared to influence the work reported in this paper.

6. Acknowledgments

The experimental work and B.M.S.C. and A.A were supported by the City of Phoenix (Sponsor Award No. 147778-0/147778-PSA-002). Support for M.A. was provided by King Abdulaziz City for Science and Technology (KACST). Support for O.A., J.P., T.V.B, and D.G. was provided by the National Alliance for Water Innovation (NAWI), funded by the U.S. Department of Energy, Office of Energy Efficiency and Renewable Energy, Advanced Manufacturing Office, under Funding Opportunity Announcement Number DE-FOA-0001905. Support for Z.M.B. was provided by discretionary funds of A.A.

7. Disclaimer

This project was funded by the United States Government.

8. References

[1] J. Yang, M. Monnot, T. Eljaddi, L. Ercolei, L. Simonian, P. Moulin, Ultrafiltration as tertiary treatment for municipal wastewater reuse, Separation and Purification Technology 272 (2021) 118921. https://doi.org/https://doi.org/10.1016/j.seppur.2021.118921.

[2] S. Al Aani, T.N. Mustafa, N. Hilal, Ultrafiltration membranes for wastewater and water process engineering: A comprehensive statistical review over the past decade, Journal of Water Process Engineering 35 (2020) 101241. https://doi.org/https://doi.org/10.1016/j.jwpe.2020.101241.

[3] A.W. Mohammad, Y.H. Teow, W.L. Ang, Y.T. Chung, D.L. Oatley-Radcliffe, N. Hilal, Nanofiltration membranes review: Recent advances and future prospects, Desalination 356 (2015) 226-254. https://doi.org/https://doi.org/10.1016/j.desal.2014.10.043.

[4] D.L. Oatley-Radcliffe, M. Walters, T.J. Ainscough, P.M. Williams, A.W. Mohammad, N. Hilal, Nanofiltration membranes and processes: A review of research trends over the past decade, Journal of Water Process Engineering 19 (2017) 164-171. https://doi.org/https://doi.org/10.1016/j.jwpe.2017.07.026.

[5] N.N.R. Ahmad, W.L. Ang, Y.H. Teow, A.W. Mohammad, N. Hilal, Nanofiltration membrane processes for water recycling, reuse and product recovery within various industries: A review, Journal of Water Process Engineering 45 (2022) 102478. https://doi.org/https://doi.org/10.1016/j.jwpe.2021.102478.

[6] L. Malaeb, G.M. Ayoub, Reverse osmosis technology for water treatment: State of the art review, Desalination 267(1) (2011) 1-8. https://doi.org/https://doi.org/10.1016/j.desal.2010.09.001.

[7] M. Wilf, S. Alt, Application of low fouling RO membrane elements for reclamation of municipal wastewater, Desalination 132(1) (2000) 11-19. https://doi.org/https://doi.org/10.1016/S0011-9164(00)00130-2.

[8] C. Fritzmann, J. Löwenberg, T. Wintgens, T. Melin, State-of-the-art of reverse osmosis desalination, Desalination 216(1) (2007) 1-76. https://doi.org/https://doi.org/10.1016/j.desal.2006.12.009.

[9] T.Y. Cath, A.E. Childress, M. Elimelech, Forward osmosis: Principles, applications, and recent developments, Journal of Membrane Science 281(1) (2006) 70-87. https://doi.org/https://doi.org/10.1016/j.memsci.2006.05.048.

[10] A. Achilli, T.Y. Cath, E.A. Marchand, A.E. Childress, The forward osmosis membrane bioreactor: A low fouling alternative to MBR processes, Desalination 239(1) (2009) 10-21. https://doi.org/https://doi.org/10.1016/j.desal.2008.02.022.

[11] Z.M. Binger, A. Achilli, Forward osmosis and pressure retarded osmosis process modeling for integration with seawater reverse osmosis desalination, Desalination 491 (2020) 114583. https://doi.org/https://doi.org/10.1016/j.desal.2020.114583.

[12] M. Hardikar, I. Marquez, A. Achilli, Emerging investigator series: membrane distillation and high salinity: analysis and implications, Environmental Science: Water Research & Technology 6(6) (2020) 1538-1552. https://doi.org/10.1039/C9EW01055F.

[13] M. Hardikar, L.A. Ikner, V. Felix, L.K. Presson, A.B. Rabe, K.L. Hickenbottom, A. Achilli, Membrane Distillation Provides a Dual Barrier for Coronavirus and Bacteriophage Removal, Environmental Science & Technology Letters 8(8) (2021) 713-718. https://doi.org/10.1021/acs.estlett.1c00483.

[14] M. Hardikar, I. Marquez, T. Phakdon, A.E. Sáez, A. Achilli, Scale-up of membrane distillation systems using bench-scale data, Desalination 530 (2022) 115654. https://doi.org/https://doi.org/10.1016/j.desal.2022.115654.

[15] D.M. Warsinger, S. Chakraborty, E.W. Tow, M.H. Plumlee, C. Bellona, S. Loutatidou, L. Karimi, A.M. Mikelonis, A. Achilli, A. Ghassemi, L.P. Padhye, S.A. Snyder, S. Curcio, C.D. Vecitis, H.A. Arafat, J.H. Lienhard, A review of polymeric membranes and processes for potable water reuse, Progress in Polymer Science 81 (2018) 209-237. https://doi.org/https://doi.org/10.1016/j.progpolymsci.2018.01.004.

[16] C. Crosson, A. Achilli, A.A. Zuniga-Teran, E.A. Mack, T. Albrecht, P. Shrestha, D.L. Boccelli, T.Y. Cath, G.T. Daigger, J. Duan, K.E. Lansey, T. Meixner, S. Pincetl, C.A. Scott, Net Zero Urban Water from Concept to Applications: Integrating Natural, Built, and Social Systems for Responsive and Adaptive Solutions, ACS ES&T Water (2020). https://doi.org/10.1021/acsestwater.0c00180.

[17] T. Wintgens, T. Melin, A. Schäfer, S. Khan, M. Muston, D. Bixio, C. Thoeye, The role of membrane processes in municipal wastewater reclamation and reuse, Desalination 178(1) (2005) 1-11. https://doi.org/https://doi.org/10.1016/j.desal.2004.12.014.

[18] C.Y. Tang, Z. Yang, H. Guo, J.J. Wen, L.D. Nghiem, E. Cornelissen, Potable Water Reuse through Advanced Membrane Technology, Environmental Science & Technology 52(18) (2018) 10215-10223. https://doi.org/10.1021/acs.est.8b00562.

[19] D. Gerrity, B. Pecson, R.S. Trussell, R.R. Trussell, Potable reuse treatment trains throughout the world, Journal of Water Supply: Research and Technology-Aqua 62(6) (2013) 321-338. https://doi.org/10.2166/aqua.2013.041.

[20] C.H. Xing, E. Tardieu, Y. Qian, X.H. Wen, Ultrafiltration membrane bioreactor for urban wastewater reclamation, Journal of Membrane Science 177(1) (2000) 73-82. https://doi.org/https://doi.org/10.1016/S0376-7388(00)00452-X.

[21] Y.H. Cai, N. Galili, Y. Gelman, M. Herzberg, J. Gilron, Evaluating the impact of pretreatment processes on fouling of reverse osmosis membrane by secondary wastewater, Journal of Membrane Science 623 (2021) 119054. https://doi.org/https://doi.org/10.1016/j.memsci.2021.119054.

[22] B.M. Souza-Chaves, M.A. Alhussaini, V. Felix, L.K. Presson, W.Q. Betancourt, K.L. Hickenbottom, A. Achilli, Extending the life of water reuse reverse osmosis membranes using chlorination, Journal of Membrane Science 642 (2022) 119897. https://doi.org/https://doi.org/10.1016/j.memsci.2021.119897.

[23] G. Huang, F. Meng, X. Zheng, Y. Wang, Z. Wang, H. Liu, M. Jekel, Biodegradation behavior of natural organic matter (NOM) in a biological aerated filter (BAF) as a pretreatment for ultrafiltration (UF) of river water, Applied Microbiology and Biotechnology 90(5) (2011) 1795-1803. https://doi.org/10.1007/s00253-011-3251-1.

[24] J.C. Crittenden, R.R. Trussell, D.W. Hand, K.J. Howe, G. Tchobanoglous, Membrane Filtration, MWH's Water Treatment: Principles and Design, Third Edition2012, pp. 819-902. https://doi.org/https://doi.org/10.1002/9781118131473.ch12.

[25] H. Gu, A. Rahardianto, L.X. Gao, X.P. Caro, J. Giralt, R. Rallo, P.D. Christofides, Y. Cohen, Fouling indicators for field monitoring the effectiveness of operational strategies of ultrafiltration as pretreatment for seawater desalination, Desalination 431 (2018) 86-99. https://doi.org/https://doi.org/10.1016/j.desal.2017.11.038.

[26] G. Fan, Z. Su, R. Lin, X. Lin, R. Xu, W. Chen, Influence of Membrane Materials and Operational Modes on the Performance of Ultrafiltration Modules for Drinking Water Treatment, International Journal of Polymer Science 2016 (2016) 6895235. https://doi.org/10.1155/2016/6895235.

[27] A.H. Nguyen, J.E. Tobiason, K.J. Howe, Fouling indices for low pressure hollow fiber membrane performance assessment, Water Research 45(8) (2011) 2627-2637. https://doi.org/https://doi.org/10.1016/j.watres.2011.02.020.

[28] S. Kasemset, L. Wang, Z. He, D.J. Miller, A. Kirschner, B.D. Freeman, M.M. Sharma, Influence of polydopamine deposition conditions on hydraulic permeability, sieving coefficients, pore size and pore size distribution for a polysulfone ultrafiltration membrane, Journal of Membrane Science 522 (2017) 100-115. https://doi.org/https://doi.org/10.1016/j.memsci.2016.07.016.

[29] E. Zondervan, B. Roffel, Evaluation of different cleaning agents used for cleaning ultra filtration membranes fouled by surface water, Journal of Membrane Science 304(1) (2007) 40-49. https://doi.org/https://doi.org/10.1016/j.memsci.2007.06.041.

[30] A.W. Zularisam, A.F. Ismail, R. Salim, Behaviours of natural organic matter in membrane filtration for surface water treatment — a review, Desalination 194(1) (2006) 211-231. https://doi.org/https://doi.org/10.1016/j.desal.2005.10.030.

[31] N. Subhi, G. Leslie, V. Chen, P. Le-Clech, Organic Fouling of Ultrafiltration Membrane: Detailed Characterization by Liquid Chromatography with Organic Carbon Detector (LC-OCD), Separation Science and Technology 48(2) (2012) 199-207. https://doi.org/10.1080/01496395.2012.686552.

[32] X. Zheng, M. Ernst, M. Jekel, Identification and quantification of major organic foulants in treated domestic wastewater affecting filterability in dead-end ultrafiltration, Water Research 43(1) (2009) 238-244. https://doi.org/https://doi.org/10.1016/j.watres.2008.10.011.

[33] M.C.V. Vela, S.Á. Blanco, J.L. García, E.B. Rodríguez, Analysis of membrane pore blocking models applied to the ultrafiltration of PEG, Separation and Purification Technology 62(3) (2008) 489-498. https://doi.org/https://doi.org/10.1016/j.seppur.2008.02.028.

[34] M. Hlavacek, F. Bouchet, Constant flowrate blocking laws and an example of their application to dead-end microfiltration of protein solutions, Journal of Membrane Science 82(3) (1993) 285-295. https://doi.org/https://doi.org/10.1016/0376-7388(93)85193-Z.

[35] N. Kalboussi, J. Harmand, A. Rapaport, T. Bayen, F. Ellouze, N. Ben Amar, Optimal control of physical backwash strategy - towards the enhancement of membrane filtration process performance, Journal of Membrane Science 545 (2018) 38-48. https://doi.org/https://doi.org/10.1016/j.memsci.2017.09.053.

[36] J.-y. Tian, M. Ernst, F. Cui, M. Jekel, Correlations of relevant membrane foulants with UF membrane fouling in different waters, Water Research 47(3) (2013) 1218-1228. https://doi.org/https://doi.org/10.1016/j.watres.2012.11.043.

[37] H. Chang, H. Liang, F. Qu, B. Liu, H. Yu, X. Du, G. Li, S.A. Snyder, Hydraulic backwashing for low-pressure membranes in drinking water treatment: A review, Journal of Membrane Science 540 (2017) 362-380. https://doi.org/https://doi.org/10.1016/j.memsci.2017.06.077.

[38] A. Touffet, J. Baron, B. Welte, M. Joyeux, B. Teychene, H. Gallard, Impact of pretreatment conditions and chemical ageing on ultrafiltration membrane performances. Diagnostic of a coagulation/adsorption/filtration process, Journal of Membrane Science 489 (2015) 284-291. https://doi.org/https://doi.org/10.1016/j.memsci.2015.04.043.

[39] Y. Zhang, Y. Sun, P. Huang, X. Zhang, Effect on water quality and control of chemically enhanced backwash by-products (CEBBPs) in the adsorption-ultrafiltration process, Water Practice and Technology 15(3) (2020) 759-772. https://doi.org/10.2166/wpt.2020.059.

[40] C. Regula, E. Carretier, Y. Wyart, G. Gésan-Guiziou, A. Vincent, D. Boudot, P. Moulin, Chemical cleaning/disinfection and ageing of organic UF membranes: A review, Water Research 56 (2014) 325-365. https://doi.org/https://doi.org/10.1016/j.watres.2014.02.050.

[41] X. Shi, G. Tal, N.P. Hankins, V. Gitis, Fouling and cleaning of ultrafiltration membranes: A review, Journal of Water Process Engineering 1 (2014) 121-138. https://doi.org/https://doi.org/10.1016/j.jwpe.2014.04.003.

[42] E. Akhondi, F. Zamani, A.W.K. Law, W.B. Krantz, A.G. Fane, J.W. Chew, Influence of backwashing on the pore size of hollow fiber ultrafiltration membranes, Journal of Membrane Science 521 (2017) 33-42. https://doi.org/https://doi.org/10.1016/j.memsci.2016.08.070.

[43] J. Kim, F.A. DiGiano, A two-fiber, bench-scale test of ultrafiltration (UF) for investigation of fouling rate and characteristics, Journal of Membrane Science 271(1) (2006) 196-204. https://doi.org/https://doi.org/10.1016/j.memsci.2005.07.027.

[44] Y. Ye, V. Chen, P. Le-Clech, Evolution of fouling deposition and removal on hollow fibre membrane during filtration with periodical backwash, Desalination 283 (2011) 198-205. https://doi.org/https://doi.org/10.1016/j.desal.2011.03.087.

[45] D.A. Waterman, S. Walker, B. Xu, R.M. Narbaitz, Bench-scale study of ultrafiltration membranes for evaluating membrane performance in surface water treatment, Water Quality Research Journal 51(2) (2016) 128-140. https://doi.org/10.2166/wqrjc.2016.039.

[46] X. Zheng, S. Plume, M. Ernst, J.-P. Croué, M. Jekel, In-line coagulation prior to UF of treated domestic wastewater – foulants removal, fouling control and phosphorus removal, Journal of Membrane Science 403-404 (2012) 129-139. https://doi.org/https://doi.org/10.1016/j.memsci.2012.02.051.

[47] J. Decarolis, S. Hong, J. Taylor, Fouling behavior of a pilot scale inside-out hollow fiber UF membrane during dead-end filtration of tertiary wastewater, Journal of Membrane Science 191(1) (2001) 165-178. https://doi.org/https://doi.org/10.1016/S0376-7388(01)00455-0.

[48] J.-J. Qin, M.H. Oo, H. Lee, R. Kolkman, Dead-end ultrafiltration for pretreatment of RO in reclamation of municipal wastewater effluent, Journal of Membrane Science 243(1) (2004) 107-113. https://doi.org/https://doi.org/10.1016/j.memsci.2004.06.010.

[49] H. Yu, X. Li, H. Chang, Z. Zhou, T. Zhang, Y. Yang, G. Li, H. Ji, C. Cai, H. Liang, Performance of hollow fiber ultrafiltration membrane in a full-scale drinking water treatment plant in China: A systematic evaluation during 7-year operation, Journal of Membrane Science 613 (2020) 118469. https://doi.org/https://doi.org/10.1016/j.memsci.2020.118469.

[50] K. Kimura, K. Kume, Irreversible fouling in hollow-fiber PVDF MF/UF membranes filtering surface water: Effects of precoagulation and identification of the foulant, Journal of Membrane Science 602 (2020) 117975. https://doi.org/https://doi.org/10.1016/j.memsci.2020.117975.

[51] H. Chang, H. Liang, F. Qu, J. Ma, N. Ren, G. Li, Towards a better hydraulic cleaning strategy for ultrafiltration membrane fouling by humic acid: Effect of backwash water composition, Journal of Environmental Sciences 43 (2016) 177-186. https://doi.org/https://doi.org/10.1016/j.jes.2015.09.005.

[52] H. Chang, H. Liang, F. Qu, S. Shao, H. Yu, B. Liu, W. Gao, G. Li, Role of backwash water composition in alleviating ultrafiltration membrane fouling by sodium alginate and the effectiveness of salt backwashing, Journal of Membrane Science 499 (2016) 429-441. https://doi.org/https://doi.org/10.1016/j.memsci.2015.10.062.

[53] S. Li, S.G.J. Heijman, J.C. van Dijk, A pilot-scale study of backwashing ultrafiltration membrane with demineralized water, Journal of Water Supply: Research and Technology-Aqua 59(2-3) (2010) 128-133. https://doi.org/10.2166/aqua.2010.053.

[54] S. Li, S.G.J. Heijman, J.Q.J.C. Verberk, A.R.D. Verliefde, A.J.B. Kemperman, J.C. van Dijk, G. Amy, Impact of backwash water composition on ultrafiltration fouling control, Journal of Membrane Science 344(1) (2009) 17-25. https://doi.org/https://doi.org/10.1016/j.memsci.2009.07.025.

[55] C. Serra, L. Durand-Bourlier, M.J. Clifton, P. Moulin, J.-C. Rouch, P. Aptel, Use of air sparging to improve backwash efficiency in hollow-fiber modules, Journal of Membrane Science 161(1) (1999) 95-113. https://doi.org/https://doi.org/10.1016/S0376-7388(99)00106-4.

[56] L. Li, H.E. Wray, R.C. Andrews, P.R. Bérubé, Ultrafiltration Fouling: Impact of Backwash Frequency and Air Sparging, Separation Science and Technology 49(18) (2014) 2814-2823. https://doi.org/10.1080/01496395.2014.948964.

[57] C. Cordier, T. Eljaddi, N. Ibouroihim, C. Stavrakakis, P. Sauvade, F. Coelho, P. Moulin, Optimization of Air Backwash Frequency during the Ultrafiltration of Seawater, Membranes 10(4) (2020) 78. https://doi.org/http://dx.doi.org/10.3390/membranes10040078.

[58] Z. Cui, J. Wang, H. Zhang, H. Jia, Influence of released air on effective backwashing length in dead-end hollow fiber membrane system, Journal of Membrane Science 530 (2017) 132-145. https://doi.org/https://doi.org/10.1016/j.memsci.2017.02.014.

[59] Y. Zhang, X. Zhao, X. Zhang, J. Sun, The influence of chemically enhanced backwash by-products (CEBBPs) on water quality in the coagulation-ultrafiltration process, Environmental Science and Pollution Research International 23(2) (2016) 1805-1819. https://doi.org/http://dx.doi.org/10.1007/s11356-015-5434-2.

[60] Y. He, J. Sharma, R. Bogati, B.Q. Liao, C. Goodwin, K. Marshall, Impacts of Aging and Chemical Cleaning on the Properties and Performance of Ultrafiltration Membranes in Potable Water Treatment, Separation Science and Technology 49(9) (2014) 1317-1325. https://doi.org/10.1080/01496395.2014.882359.

[61] S. Delgado Diaz, L. Vera Peña, E. González Cabrera, M. Martínez Soto, L.M. Vera Cabezas, L.R. Bravo Sánchez, Effect of previous coagulation in direct ultrafiltration of primary settled municipal wastewater, Desalination 304 (2012) 41-48. https://doi.org/https://doi.org/10.1016/j.desal.2012.08.005.

[62] K. Kimura, Y. Hane, Y. Watanabe, Effect of pre-coagulation on mitigating irreversible fouling during ultrafiltration of a surface water, Water Science and Technology 51(6-7) (2005) 93-100. https://doi.org/10.2166/wst.2005.0626.

[63] B.-B. Lee, K.-H. Choo, D. Chang, S.-J. Choi, Optimizing the coagulant dose to control membrane fouling in combined coagulation/ultrafiltration systems for textile wastewater

reclamation, Chemical Engineering Journal 155(1) (2009) 101-107. https://doi.org/https://doi.org/10.1016/j.cej.2009.07.014.

[64] K.Y.-j. Choi, B.A. Dempsey, In-line coagulation with low-pressure membrane filtration, Water Research 38(19) (2004) 4271-4281. https://doi.org/https://doi.org/10.1016/j.watres.2004.08.006.

[65] L.X. Gao, H. Gu, A. Rahardianto, P.D. Christofides, Y. Cohen, Self-adaptive cycle-to-cycle control of in-line coagulant dosing in ultrafiltration for pre-treatment of reverse osmosis feed water, Desalination 401 (2017) 22-31. https://doi.org/https://doi.org/10.1016/j.desal.2016.09.024.

[66] K.B. Newhart, R.W. Holloway, A.S. Hering, T.Y. Cath, Data-driven performance analyses of wastewater treatment plants: A review, Water Research 157 (2019) 498-513. https://doi.org/https://doi.org/10.1016/j.watres.2019.03.030.

[67] M.C. Klanderman, K.B. Newhart, T.Y. Cath, A.S. Hering, Case studies in real-time fault isolation in a decentralized wastewater treatment facility, Journal of Water Process Engineering 38 (2020) 101556. https://doi.org/https://doi.org/10.1016/j.jwpe.2020.101556.

[68] K.B. Newhart, J.E. Goldman-Torres, D.E. Freedman, K.B. Wisdom, A.S. Hering, T.Y. Cath, Prediction of Peracetic Acid Disinfection Performance for Secondary Municipal Wastewater Treatment Using Artificial Neural Networks, ACS ES&T Water 1(2) (2021) 328-338. https://doi.org/10.1021/acsestwater.0c00095.

[69] S. Chellam, N.G. Cogan, Colloidal and bacterial fouling during constant flux microfiltration: Comparison of classical blocking laws with a unified model combining pore blocking and EPS secretion, Journal of Membrane Science 382(1) (2011) 148-157. https://doi.org/https://doi.org/10.1016/j.memsci.2011.08.001.

[70] W. Yuan, A. Kocic, A.L. Zydney, Analysis of humic acid fouling during microfiltration using a pore blockage–cake filtration model, Journal of Membrane Science 198(1) (2002) 51-62. https://doi.org/https://doi.org/10.1016/S0376-7388(01)00622-6.

[71] J.C. Schippers, J. Verdouw, The modified fouling index, a method of determining the fouling characteristics of water, Desalination 32 (1980) 137-148. https://doi.org/https://doi.org/10.1016/S0011-9164(00)86014-2.

[72] E. Iritani, A Review on Modeling of Pore-Blocking Behaviors of Membranes During Pressurized Membrane Filtration, Drying Technology 31(2) (2013) 146-162. https://doi.org/10.1080/07373937.2012.683123.

[73] E. Iritani, N. Katagiri, T. Takenaka, Y. Yamashita, Membrane pore blocking during cake formation in constant pressure and constant flux dead-end microfiltration of very dilute colloids, Chemical Engineering Science 122 (2015) 465-473. https://doi.org/https://doi.org/10.1016/j.ces.2014.09.052.

[74] N. Porcelli, S. Judd, Chemical cleaning of potable water membranes: A review, Separation and Purification Technology 71(2) (2010) 137-143. https://doi.org/https://doi.org/10.1016/j.seppur.2009.12.007.

[75] E.W. Tow, A.L. Hartman, A. Jaworowski, I. Zucker, S. Kum, M. AzadiAghdam, E.R. Blatchley, A. Achilli, H. Gu, G.M. Urper, D.M. Warsinger, Modeling the energy consumption of potable water reuse schemes, Water Research X 13 (2021) 100126. https://doi.org/https://doi.org/10.1016/j.wroa.2021.100126.